

## Recent developments in background oriented schlieren methods for rotor blade tip vortex measurements

Kolja Kindler<sup>1</sup>, Erik Goldhahn<sup>2</sup>, Friedrich Leopold<sup>3</sup>, Markus Raffel<sup>1</sup>

- 1: German Aerospace Center (DLR) Institute for Aerodynamics and Flow Technology, Göttingen, Germany, kolja.kindler@dlr.de, markus.raffel@dlr.de  
2: University of Hannover, Institute for Turbo Machinery and Fluid Dynamic (TFD), Hannover, Germany, goldhahn@tfd.uni-hannover.de  
3: Institute Franco-Allemand de Recherche de Saint-Luis (ISL), Saint-Luis, France, leopold@isl.tm.fr

---

**Abstract** Compressible blade tip vortices (BTV) of rotary wings have been subject of numerous investigations and their importance for the understanding of the helicopter flow field has clearly been drawn. Due to its great impact on the dynamics of the flow field, the investigation of the BTV is directly linked to issues of flow control and aeroacoustic optimization. However, despite of the velocity field data of the BTV, additional density information for vortex modeling is desirable. In this work we briefly describe the set up of an airborne background oriented optical stereoscopic schlieren (BOSS) system for helicopter flight tests as well as preliminary experimental results of background oriented optical tomography (BOOT) of a 0.4 Mach scaled rotor model investigation. The tomographic approach enabled us computing an estimate of the tip vortex density field. This method is demonstrated to yield reasonable scales of the vortex core diameter. The advantages and applicability of the filtered back-projection method for rotor investigations will be discussed.

---

### Nomenclature

$C_T$	thrust coefficient	$x, y, z$	cartesian coordinates
$c$	blade chord length		
$D$	Gladstone-Dale constant	$\gamma$	deflection angle
$k_{x,y}$	spatial frequencies	$\delta z$	image distortion
$Ma$	Mach number	$\delta\rho$	density variation
$n$	index of refraction	$\rho$	density
$R$	blade radius	$\Theta$	projection angle
$r_c$	core radius	$\sigma$	solidity

## 1. Introduction

The tip vortex shed from revolving helicopter rotor blades is a compressible sharply localized vortical structure whose strength and structure is known to depend on the blade tip Mach and Reynolds number (see e.g. McCroscey (1995), Leishman (1998)). Depending on the flight path, the relative distance and orientation of the vortex of a preparatory blade and the successive one, blade-vortex interactions (BVI) might occur, which are considered a major source of aeroacoustic noise in rotor flight. Especially in low-speed descending flight or maneuvers the sound emission as well as structural vibrations increase remarkably. Therefore, numerous experimental studies of the rotor flow field and the BVI have been conducted mostly employing optical measurement techniques (e.g. van der Wall and Richard (2005) and Richard et al (2006)). Beside the experimental approach, numerical simulation and corresponding aeroacoustic modeling of both the near and the far field are increasingly important tools in the investigation of helicopter aerodynamics Ehrenfried et al (1991), Strawn et al

(1996). However, due to the complexity of the flow field, numerical investigations might be improved considerably by the support of experimental data on the density in the vortex core.

On the other hand, direct density measurements at the blade tip so far reported are mostly complicated and time consuming. Interferometric techniques for example rely on optical arrangements and lasers restricting those techniques to the laboratory use only (see for example Snyder and Hesselink (1984), Chandrasekhara et al (1995)). Therefore, it seems to be proximate to apply the Background Oriented Schlieren (BOS) technique with a view to BTV detection.

Commonly, the BOS technique is based on directly imaging a white light speckle pattern with and without an aerodynamic structure influencing the light path. The density gradients, introduced by a compressible and distinctively localized vortex for example, are related to gradients of the refractive index which are transferred into a deformation of the imaged background pattern. Hence, the vortex structure morphology can be reconstructed based on the an image-reference pair using robust and very efficient cross-correlation methods. For a detailed description of the BOS technique we refer to Dalziel et al (2000) and Raffel et al (2000).

Furthermore, implying a vortex such as the BTV to be rotational symmetric, the density field might be estimated based on BOS data. This recording technique, an it combination with the tomographic evaluation will be referred to as background oriented optical tomography (BOOT). As according to previous investigations (see e.g. Richard et al (2006)) the BTV sufficiently matches this symmetry condition<sup>1</sup>, we use the filtered back-projection method applied to slices of two-dimensional background image data of hovering in ground effect in order to derive a density field estimate of the cross-section of the BTV. Since the BOOT data has been obtained very recently, it has to be regarded as preliminary, we do not attempt to quantitatively compare our results to the literature available but we emphasize the applicability of the evaluation scheme. A careful analysis of hot air jet calibration data, that has been taken directly after test in the facility should allow later validation of the results obtained.

Briefly outlining the organization of the article, we will depict the Filtered back-projection algorithm in the next section and specify the experimental details of the work thereafter. Subsequently, we report the results of the tomographic evaluation and summaries the main conclusions.

## 2. Tomographic evaluation

Adopting the deflections of the light rays passing a density gradient to be sufficiently small the deflection angles  $\gamma_{x,y}$  read:

$$\tan(\gamma_{x,z}) = \int \frac{\partial \rho}{\partial(x,z)} dy \quad . \quad (1)$$

The deflection might be regarded as the Radon transform of the density gradient field with respect to the line of sight. The Radon transform itself is well-known in medical tomographic imaging application and one might refer to Toft (1996) for a comprehensive review.

In Fig. 1 we sketch a slice of the density field of an idealized vortex. Introducing a coordinate system  $(x',y')$  wherein the line of sight is parallel to the  $y'$ -axis (see Fig. 1 on the left), the Radon transform of the density along the line of sight takes the form:

$$R\{\rho\}(x',\Theta) = \int_{-\infty}^{\infty} \rho(x,y) dt$$

---

<sup>1</sup>The rotational symmetry of the BTV alludes to “young” vortices, in the close vicinity of the blade’s trailing edge.

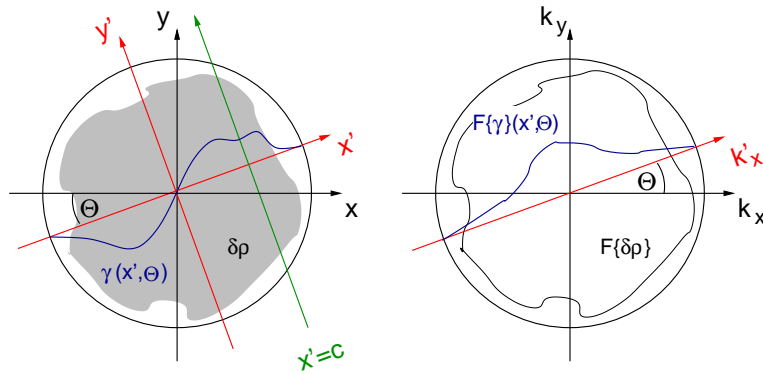


Figure 1: On the interpretation of the tomographic algorithm, a slice of a rotational symmetric density variation in physical (left) and Fourier space (right). The green line on the right represents the path of an example ray passing the density structure. See the text for further details.

$$= \int_{-\infty}^{\infty} \rho(x' \cdot \cos(\Theta) - y' \cdot \sin(\Theta), y' \cdot \cos(\Theta) + x' \cdot \sin(\Theta)) dy' \quad (2)$$

and the corresponding Fourier transform of  $R\{\rho\}$

$$\begin{aligned} F\{R\{\rho\}\}(k'_x, \Theta) &= \int_{-\infty}^{\infty} \int_{-\infty}^{\infty} \rho(x' \cdot \cos(\Theta) - y' \cdot \sin(\Theta), \dots \\ &\quad y' \cdot \cos(\Theta) + x' \cdot \sin(\Theta)) \cdot e^{-i2\pi k'_x x'} dy' dx' \\ &\equiv \aleph(k'_x, \Theta) \quad , \end{aligned} \quad (3)$$

which is sketched in Fig. 1 also.

The Fourier transform of the deflection angles

$$\begin{aligned} F\{\gamma\}(k'_x, \Theta) &= \int_{-\infty}^{\infty} \gamma(x', \Theta) \cdot e^{-i2\pi k'_x x'} dx' \\ &= D \int_{-\infty}^{\infty} \int_{-\infty}^{\infty} \frac{\partial \rho}{\partial x'} \cdot e^{-i2\pi k'_x x'} dy' dx' \\ &= D \cdot i \cdot 2\pi \cdot k'_x \cdot \aleph(k'_x, \Theta) \\ &\equiv \Gamma(k'_x, \Theta) \end{aligned} \quad (4)$$

with  $D$  being the Gladstone-Dale constant, leads to the relation of the deflection angles and the Radon transform of the density. Inverting the Fourier transform of  $R\{\rho\}$  using polar coordinates one writes

$$\rho(x, y) = \rho(x' \cdot \cos(\Theta) - y' \cdot \sin(\Theta), y' \cdot \cos(\Theta) + x' \cdot \sin(\Theta))$$

$$\begin{aligned}
 &= \int_0^{2\pi} \int_0^{\infty} \mathfrak{N}(k'_x, \Theta) \cdot e^{i2\pi \cdot k'_x \cdot x'} dy' dx' \\
 \rho(x,y) &= \int_0^{\pi} \int_{-\infty}^{\infty} \mathfrak{N}(k'_x, \Theta) \cdot |k'_x| \cdot e^{i2\pi \cdot k'_x \cdot x'} dy' dx' \\
 &= \int_0^{\pi} \int_{-\infty}^{\infty} \underbrace{\frac{|k'_x|}{D \cdot i \cdot 2\pi \cdot k'_x}}_{\equiv Q(k'_x)} \cdot \Gamma(k'_x, \Theta) \cdot e^{i2\pi \cdot k'_x \cdot x'} dy' dx' \quad (5)
 \end{aligned}$$

wherein  $Q$  is a filter applied to  $\Gamma$  in Fourier space. Equation 5 basically resembles the Fourier slice theorem.

Taking into account the convolution theorem Eqn. 5 is equivalent to:

$$\rho(x,y) = \int_0^{\pi} q(x') * \gamma(x', \Theta) d\Theta \quad (6)$$

with

$$q(x') = F^{-1}\{Q(k'_x, \Theta)\} \quad \text{and} \quad \gamma(x', \Theta) = F^{-1}\{\Gamma(k'_x, \Theta)\} \quad .$$

Henceforth, we are able to specify the density field based on the image deflections measured and the known distance of the vortex. Filtering the deflection angles with  $Q(k'_x)$  in Fourier space and computing the inverse transformation yields the density field data.

### 3. Experiments at model scale

The experimental setup in the rotor testing hall of DLR Braunschweig is the same as described by Richard et al (2006). A 40% dynamically Mach-scaled model of the MBB BO-105 main rotor was used ( $R = 2$  m and  $c = 0.121$  m chord length). The blades possess a  $2.5^\circ$  pre-cone at the hub and a rectangular plan form featuring  $-8^\circ/R$  linear twist at a solidity of  $\sigma = 0.077$ . The BOS results to be presented refer to the rotor operating in ground effect at tip Mach numbers of  $Ma = 0.633$  and at thrust coefficients of  $C_T = 0.0028$ .

The BOS setup consisted of a PCO SensiCam in connection with a 300 mm lens observing a homogeneously illuminated speckle pattern from above the rotor plane. The camera was positioned at a distance of  $3.289R$  with respect to the measurement volume with the background being another  $5.289R$  away. The extension of the imaging plane is  $1024 \times 1280$  px<sup>2</sup> with a resolution of approximately 7.34 px/mm. Subsequently, the raw data was processed using PivView.

### 4. Set up of the airborne BOSS system

An airborne camera system has been set up for first full-scale flight tests on a BO 105 helicopter. The basic idea was to setup a very simple hand-held device which allows for dynamic reference-free data acquisition associated with natural formations as BOS background. The underlying principle of the reference-free BOSS technique is described in Raffel et al (2000). A non-correlating but homogeneous natural scenery such as grass or leaves can provide the required background for the BOSS technique (see. e.g. Richard and Raffel (2001)). We used leaves of a skirt of wood in order to take

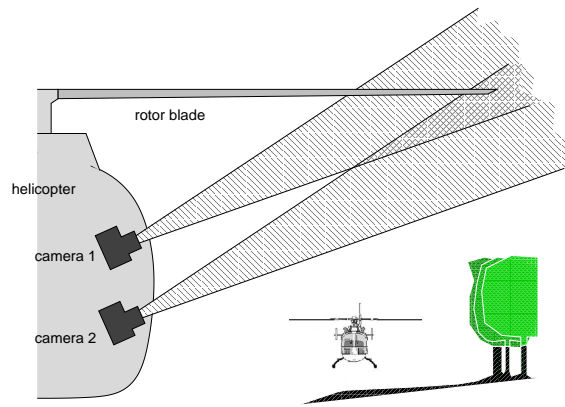


Figure 2: Sketch of the full-scale in-flight experiment utilizing skirts of wood as a natural background for reference-free stereoscopic BOS.

advantage of their color depth and large contrast. Furthermore, Gruppi et al (2005) introduced a procedure to apply weighted local color separation thereby gaining an increase of the signal-to-noise ratio, which is also capable of artificially shrinking larger structures of the background. The main restriction for the in-flight imaging from within the fuselage with a view to BOSS is the fairly short and fixed distance between camera and vortex. As the image displacement is expected to be rather weak, one cannot compensate for that by large image distances. Thus, the images of the stereoscopic system must be aligned very carefully as well as their resolution has to allow for comparatively small evaluation window sizes.

The airborne BOSS system consisted of two high resolution Canon OES 1Ds Mark II cameras with a 70 to 200 mm zoom objective mounted on an X95 profile, aligned vertically and placed behind the co-pilot's seat (Fig. 2). The sensor unit remained flexible during the test in order to manually direct to the blade tip position. The BO 105 has a main rotor radius of  $R=4.98$  m and a chord length of  $R=0.2$  m. The images were recorded at approximately 2 px/mm and 11 px/mm resolution with the 70 mm and 200 mm objective respectively. The viewing axis of the cameras were adjusted to be parallel and the spacing in between has been optimized in order to gain an image separation of  $0.5c$  in the blade tip plane. The distance between the cameras and the expected tip vortex position was approximately  $R$  while the distance to the background varied between 20–100 m. The measurements were conducted in very low-level hover flight at an altitude less than  $R$ .

## 5. Results

Figure 3 shows an example of a BOSS result of the BTV in the vicinity of the blade. The main deflections are observed in the  $y$ -component, while the chordwise  $x$ -component turns out to be fairly noisy. However, the vortex is fully developed at the trailing edge and starts to spread increasing its core radius at approximately  $z \approx 0.5c$ . We note that due to limitations of the light intensity mainly determining the exposure time, the BOS data is biased by smear effects of the blade. The area of cohesive positive in-plane deflection magnitude closely above the blade tip is probably an artefact of smearing ((0, -0.1) in Fig. 3 corresponds to the position of the trailing edge of the blade tip). Therefore, the instantaneous BOS results imply a spatial average of approximately  $5^\circ$  and additionally a conditional average is calculated from series of ten images in order to enhance the signal. These averaged fields are evaluated by means of filtered back-projection at three different chordwise positions. Considering these averaging effects smearing the narrow vortex core, we expect the density to be underestimated

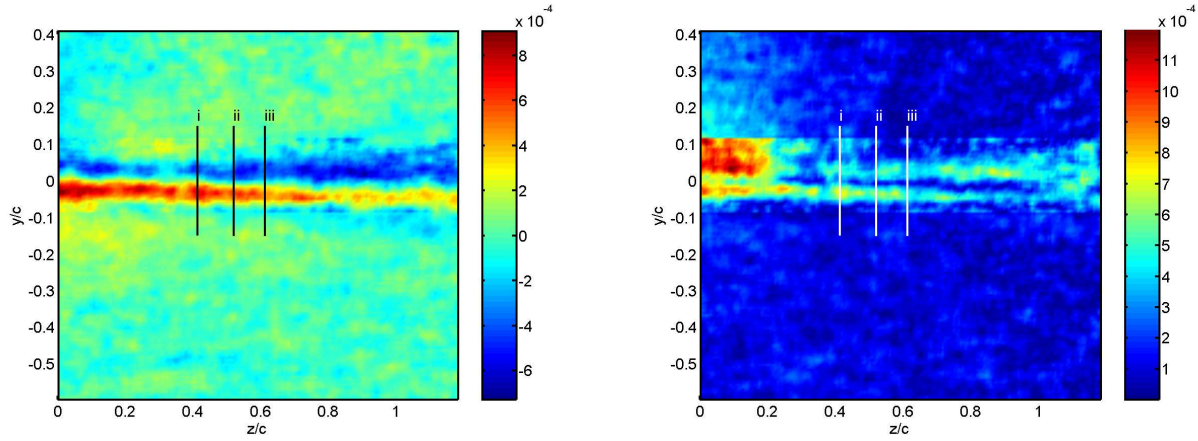


Figure 3: Image displacement (mm) of the  $y$ -component (left) and the in-plane magnitude of displacement (mm) (right) of the BTV at  $Ma=0.633$  and  $C_T=0.0049$ .

by the back-projection scheme in addition to effects of the limited spatial resolution.

Figure 4 depicts the deflection data analyzed (sliced at the positions  $i, ii$  and  $iii$  in Fig. 3) and the corresponding density estimates. The three slices are extracted from the field data at  $0.41c$ ,  $0.52c$  and  $0.61c$  downstream the trailing edge of the blade. The vortex structure can clearly be identified,

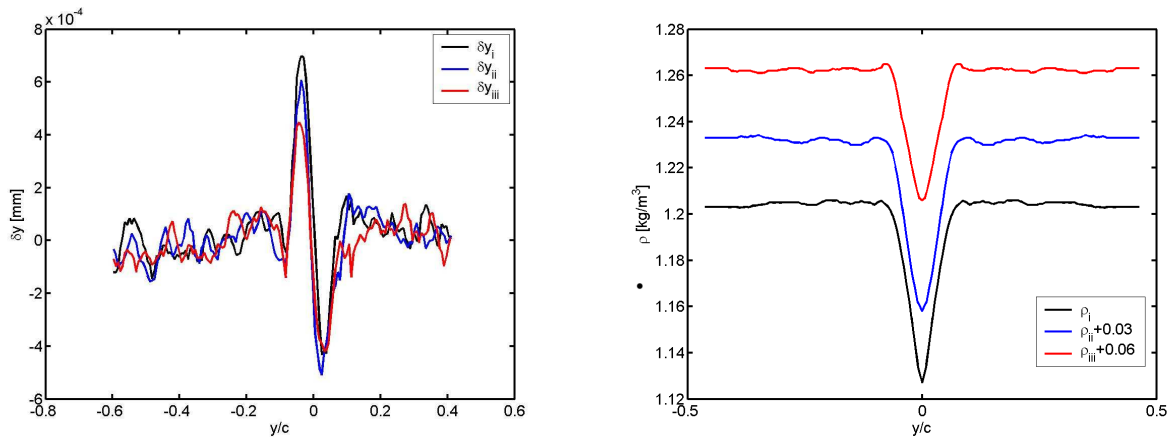


Figure 4: Image displacement of the  $y$ -component (left) and the corresponding density estimates (right) at the three positions given in Fig. 3. The density is azimuthal averaged with respect to the vortex core position in the  $y$ - $z$ -plane.

although the deflections are not symmetric at all three positions. We mainly attribute this lack of symmetry to small camera deflections resulting from the air loads during the rotor run.

Application of filtered back-projection implying standard atmospheric conditions and  $T = 20^\circ\text{C}$  yields the density shown on the right of Fig. 4 exhibiting central core density drops of the order of 10% slightly decreasing with increasing distance from the trailing edge and the onset of lateral swelling. The limited density drop can be identified with the effects of smearing already quoted above. A vortex core diameter in the order of  $r_c \approx 0.05 \cdot c$  can be expected based on velocity measurements (see e.g. van der Wall and Richard (2005)). The density distribution we estimate has an extension of approximately  $0.20c$  which is slightly larger than the velocity based value of the core given above.

With a view to our first flight test with the airborne system, we note that the light intensity essential to acquire BOS data of adequate resolution turns out to be a severe issue. Although the measurements profited from sunny and cloudless conditions, we had to reduce to the 70 mm-lens in order to suppress smearing of the blade.

The low resolution of the 70 mm-lens images strongly hampers the data evaluation, because of the very narrow evaluation windows necessary to unambiguously identify the vortex.

However, we realized that the leave density and remainders of tree trunks demands further post-processing of the images.

## 6. Conclusions

Background images through the tip vortex in the vicinity of the rotor blade have been recorded on a 40% Mach-scaled rotor model of the BO 105. The recordings have been evaluated utilizing the filtered back-projection method. The vortex core diameter found is on reasonable scales while the extent of the density drop within the vortex core remains under-estimated. However, we demonstrated the evaluation of planar BOS data with the aid of a tomographic algorithm to be successfully applicable to young blade tip vortices.

Furthermore, the full-scale in-flight measurements with the BO-105 test-helicopter in hover flight are reported. Utilizing a hand-held stereoscopic BOS system we recorded the blade tips with various magnifications from the fuselage. More work has to be done in order to improve the tolerance of the technique with respect to a background topology that is not planar but has a limited three-dimensionality.

Although, the full-scale application is hampered by various difficulties and limitations, in-flight measurements and subsequent core density estimations are a promising task aiming at full Reynolds number vortex data that might be obtained at various flight conditions.

## References

- Chandrasekhara M, Squires D, Wilder M, Carr L (1995) A phase-locked high-speed real-time interferometry system for large amplitude unsteady flows. *Exp Fluids* 20(2):61
- Dalziel S, Hughes G, Sutherland B (2000) Whole-field density measurements by 'synthetic schlieren'. *Exp Fluids* 28:322
- Ehrenfried K, Meier G, Obermeier F (1991) Sound produced by vortex-airfoil interaction. In: 17th ERF, Berlin, Germany
- Gruppi D, Guernier S, Leopold F, Schäfer H (2005) Mehrfarben-Hintergrund-schlieren-Technik (CBOS) zur Vermessung der Lichtablenkung von Dichtegradienten. In: Fachtagung Lasermethoden in der Strömungsmechanik, Sep. 6-8th 2005, BTU Cottbus (in german)
- Leishman J (1998) Measurement of the aperiodic wake of a hovering rotor. *Exp Fluids* 25:352
- McCroscey W (1995) Vortex wake of rotor craft. In: 33th AIAA Aerospace Science Meeting and Exhibit, Reno, USA
- Raffel M, Tung C, Richard H, Yu Y, Meier G (2000) Background oriented stereoscopic schlieren (boss) for full scale helicopter vortex characterization. In: 9th Int. Symp. on Flow Visualization, Heriot-Watt University, Edinburgh, G.B.

- Richard H, Raffel M (2001) Visualization of vortical structures by density gradient detection. In: PSFVIP-3, June 18-21 2001, Maui, Hawaii, U.S.A.
- Richard H, Bosbach J, Henning A, Raffel M, van der Wall B (2006) 2c and 3c piv measurements on a rotor in hover condition. In: 13th Int. Symp. on Applications of Laser Techniques to Fluid Mechanics, 26-29th June, Lisbon, Portugal
- Snyder R, Hesselink L (1984) Optical tomography for flow visualization of the density field around a revolving helicopter blade. *Appl Optics* 23(20):3650
- Strawn R, Oliker L, Biswas R (1996) New computational methods for the prediction and analysis of helicopter noise. In: 2nd AIAA/CEAS Aeroacoustic Conference, May 1996, State College, PA, USA
- Toft P (1996) The radon transform, theory and implementation. Ph.D. thesis, Technical University of Denmark, Kogens Lyngby, Denmark
- van der Wall B, Richard H (2005) Visualization of vortical structures by density gradient detection. In: The 2nd Int. Basic Research Conference on Rotorcraft Technology, Nov 7-9th, Nanjing, China